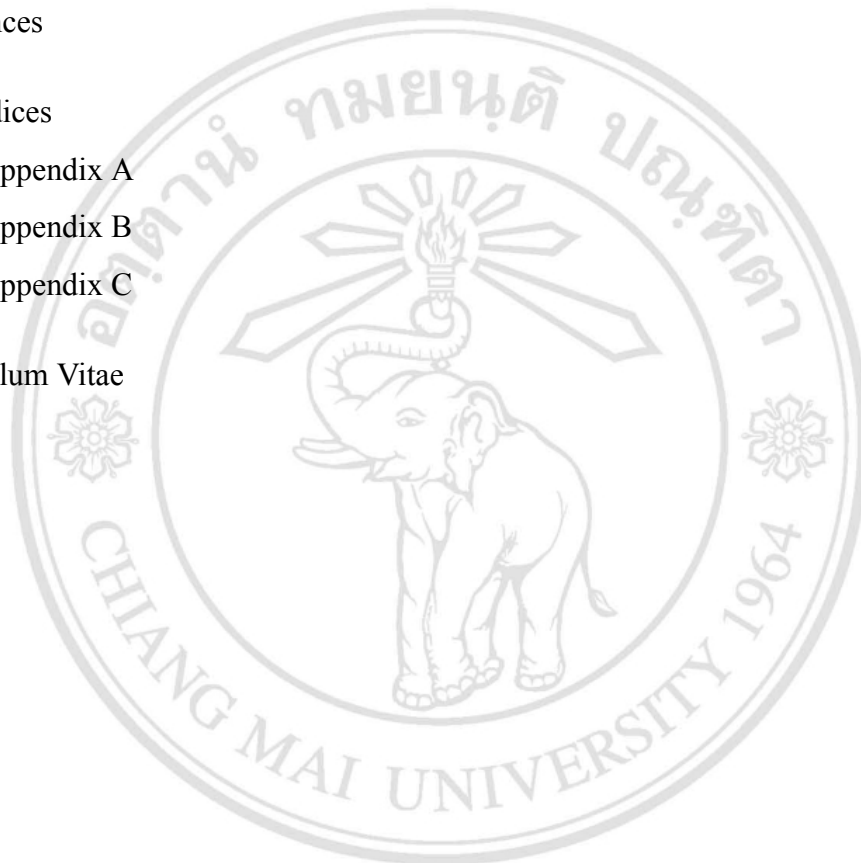


# CONTENTS

	Page
Acknowledgement	d
Abstract in Thai	e
Abstract	g
List of Tables	k
List of Figures	n
Chapter 1 Introduction	1
Chapter 2 Drift Chamber Principal of Operation	6
2.1 Basic Components	6
2.2 Ionization of the Gas Molecules	8
2.3 Drift of Electrons	12
2.4 Gas Amplification	13
2.5 Signal Generation	16
2.6 The Impact Factors on Spatial Resolution	16
Chapter 3 Inner Part of Belle II Central Drift Chamber	19
3.1 Core Structure	19
3.2 Wire Configuration	21
Chapter 4 Assembling of Inner Part of Belle II CDC	25
4.1 Core Structure Assembling and Tension Load Test	25
4.2 Wire Stringing	28
4.3 Wire Tension Measurement	30
4.4 Gas Leak Test	32

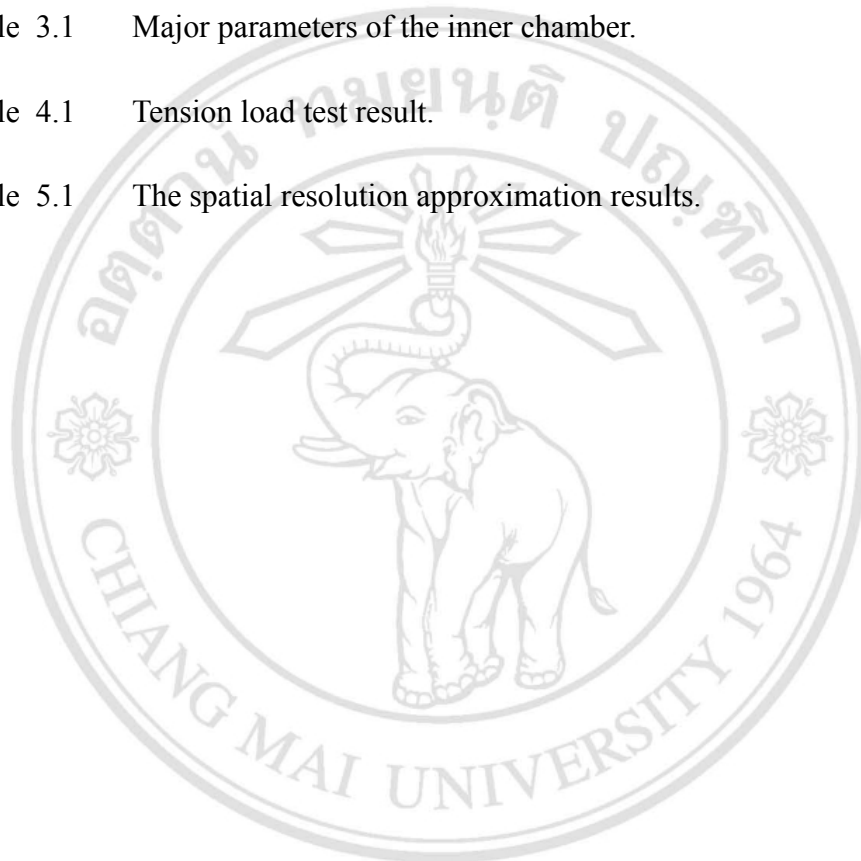
Chapter 5	Cosmic Ray Test	36
5.1	Detector Setup	36
5.2	Raw Data Interpretation	40
5.3	Spatial Resolution Approximation	62
Chapter 6	Conclusion	69
References		71
Appendices		73
Appendix A		74
Appendix B		76
Appendix C		77
Curriculum Vitae		78



ลิขสิทธิ์มหาวิทยาลัยเชียงใหม่  
Copyright© by Chiang Mai University  
All rights reserved

## LIST OF TABLES

	Page
Table 3.1 Major parameters of the inner chamber.	21
Table 4.1 Tension load test result.	26
Table 5.1 The spatial resolution approximation results.	67



ลิขสิทธิ์มหาวิทยาลัยเชียงใหม่  
Copyright© by Chiang Mai University  
All rights reserved

# LIST OF FIGURES

	Page
Figure 1.1 Schematic diagram of the SuperKEKB upgrade	3
Figure 1.2 Layout of the Belle II detector components	3
Figure 1.3 A reconstructed tracks of the charged particles from the Belle experiment	4
Figure 2.1 A model of a drift chamber	7
Figure 2.2 Drift the chamber principle of operation	9
Figure 2.3 The expected curve of the energy loss as a function of momentum(P)	10
Figure 2.4 The energy loss distribution in an argon-carbon dioxide counter	11
Figure 2.5 Diagram of Avalanche process	14
Figure 2.6 Plot of the number of the generated electron-ion pairs as a function of the gain-voltage	15
Figure 2.7 Measured spatial resolution at incident angle of $90^\circ$ as a function of distance from the sense wire. The histogram shows the residual at the whole region of the drift distance. The resolution derived from this experiment is $120 \mu\text{m}$ .	17
Figure 2.8 The decomposition of the residual distribution as a function of the drift distance.	18
Figure 3.1 Main structure of the Belle II CDC	20
Figure 3.2 Layout of inner chamber of the Belle II CDC	20
Figure 3.3 Detailed layout of inner chamber in close-up view	21
Figure 3.4 Layout of wire configuration of the Belle II drift chamber.	23
Figure 3.5 The stereo wire diagram.	23
Figure 3.6 Assembled core structure of the Belle II CDC inner chamber	24

Figure 4.1	Plot of the length difference between before and after the tension applied (mm) and tension (kg)	26
Figure 4.2	The chamber set up for tension load test.	27
Figure 4.3	Three different types of feed through	28
Figure 4.4	Three difference types of feed through	29
Figure 4.5	The sense wire stringing	30
Figure 4.6	The Inner Chamber with the whole wires strung	31
Figure 4.7	Setup for the tension measurement	32
Figure 4.8	Gas leak test	34
Figure 4.9	Improvement of the gas leak rate	35
Figure 5.1	The overview of the detector setup for the cosmic ray detection	37
Figure 5.2	The diagram of the detector setup for trigger signal generating	38
Figure 5.3	The time measurement procedure	40
Figure 5.4	The raw data format	42
Figure 5.5	The procedure of the generated charge analysis	43
Figure 5.6	The FADC summation distribution (ch. 0 - 5).	44
Figure 5.7	The FADC summation distribution (ch. 6 - 11).	45
Figure 5.8	The FADC summation distribution (ch. 12 - 17).	46
Figure 5.9	The FADC summation distribution (ch. 18 - 23).	47
Figure 5.10	The FADC summation distribution (ch. 24 - 29).	48
Figure 5.11	The FADC summation distribution (ch. 30 - 36).	49
Figure 5.12	The FADC summation distribution (ch. 37 - 42).	50
Figure 5.13	The FADC summation distribution (ch. 43 - 47).	51
Figure 5.14	The distribution of the amount of hit times per channel	52
Figure 5.15	An example of TDC distribution for one channel	53
Figure 5.16	The drift time distribution (ch. 0 - 5).	54
Figure 5.17	The drift time distribution (ch. 6 - 11).	55
Figure 5.18	The drift time distribution (ch. 12 - 17).	56
Figure 5.19	The drift time distribution (ch. 18 - 23).	57
Figure 5.20	The drift time distribution (ch. 24 - 29).	58

Figure 5.21	The drift time distribution (ch. 30 - 36).	59
Figure 5.22	The drift time distribution (ch. 37 - 42).	60
Figure 5.23	The drift time distribution (ch. 43 - 47).	61
Figure 5.24	The distribution of the amount of good timing drift cell per event	62
Figure 5.25	An example of drift time distribution with its, minimum drift time, $T_0$ , and maximum drift time, $T_{max}$ .	63
Figure 5.26	The X-T relation plot of layers 1 to 4.	65
Figure 5.27	The X-T relation plot of layers 5 to 8.	66
Figure 5.28	An example of the cosmic ray reconstructed track.	67
Figure 5.29	An example of the residual distribution of the layer number 6 with the Gaussian fit.	68
Figure B.1	the measured drift velocity of the 50% $He$ - 50% $C_2H_6$ mixture.	76